IGARSS 2024 - 2024 IEEE International Geoscience and Remote Sensing Symposium | 979-8-3503-6032-5/24/$31.00 ©2024 IEEE | DOI: 10.1109/IGARSS53475.2024.10640409

CALIBRATION OF THE AIRBORNE POLARIMETRIC GNSS-R SENSOR FOR THE RONGOWAI PROJECT

Dinan Bai[1], Chris Ruf[1], Andrew O'Brien[2], Delwyn Moller[3]

1. University of Michigan, Department of Climate and Space Sciences and Engineering
2. The Ohio State University, ElectroScience Laboratory
3. University of Auckland, Department of Electrical. Computer and Software Engineering

ABSTRACT

This paper presents the calibration process for an airborne polarimetric Global Navigation Satellite System Reflectometry (GNSS-R) sensor developed for the Rongowai project. We calibrate the sensor's dual-polarized antenna pattern and power measurement by comparing field data obtained from an inland lake surface with model predictions. The model evaluates the dual-polarized power of coherent polarimetric GPS signals reflected from inland water body surfaces with slight roughness caused by winds. The calibration results suggest a rotation of the polarimetric antenna gain pattern. A different scale factor is applied to the system's dual-polarized power measurement for 1 and 2 millisecond coherent integration times. The absolute power calibration allows accurate surface reflectivity and normalized bistatic radar cross section (NBRCS) retrieval and enables future science applications.

Index Terms—Remote Sensing, Polarimetric GNSS-R, Calibration

1. INTRODUCTION

Global Navigation Satellite System Reflectometry (GNSS-R) measures GNSS signals scattered from the earth surface for remote sensing applications. Spaceborne GNSS-R has been investigated in satellite missions such as UK-DMC [1] and TDS-1 [2] launched in 2004 and 2014 respectively. The NASA Cyclone Global Navigation Satellite System Earth Venture mission (CYGNSS) [3] was launched in 2016 and measures surface windspeed in tropical cyclones to improve storm forecasting. An empirical approach based on the normalized bistatic radar cross section (NBRCS) is used in the CYGNSS ocean windspeed retrieval [4]. Accurate knowledge of NBRCS requires absolute calibration of the received power. The calibration parameters include accurate measurements of GPS Equivalent Isotropic Radiated Power (EIRP) and the receiver's antenna gain pattern [5,6]. The absolute calibration of GNSS-R not only supports ocean windspeed retrievals but also provides physical insights into the scattering mechanism on the earth surface and helps to extend CYGNSS applications to land surface remote sensing. Besides NBRCS, calibrated received power can be used to retrieve land surface reflectivity. Studies have demonstrated the sensitivity of spaceborne GNSS-R to surface reflectivity which is directly related to inland waterbody extent and near-surface soil moisture [7]. It should be noted that only the co-pol scattering process is considered in these earlier studies since the associated satellite missions were equipped with antennas of a single polarization.

At spaceborne altitudes and velocities, delay and doppler bins correspond to surface areas of hundreds of km^2 resulting in a high likelihood of non-uniform wind fields within the spatial resolution cell. In comparison airborne experiments have greatly enhanced spatial resolutions, airborne experiments [8] demonstrated right hand circularly polarized (RHCP) GPS signals reflected from the ocean surface were cross-correlated with a local replica of the GPS PRN code to create Delay Doppler Maps (DDMs) whose pixels are proportional to the scattered power from the surface. The shape of the delay waveform of the DDM, including the trailing edge slope and full waveform, are used [9] to retrieve ocean surface roughness and windspeed with a spatial resolution of several kilometers. Absolute calibration of the received power is not required in the waveform-shape-based approaches because the retrieval only depends on the relative shape of the waveform.

Seeking better coverage, resolution, and geophysical retrievals accuracy to enhance GNSS-R capability, NASA, New Zealand's Ministry of Business Innovation and Employment, the University of Michigan, the University of Auckland and Air New Zealand initiated an airborne project called "Rongowai" in 2022 [10] to support the calibration and validation component of the current CYGNSS mission. A newly developed Next Generation GNSS-R Receiver (NGRx) is installed on a domestic Air New Zealand aircraft to collect data. Compared with traditional GNSS-R systems, the NGRx has the capabilities of processing multi-GNSS-satellite signals simultaneously with a Co-pol and Cross-pol dual-channel antenna to achieve better spatial coverage and retrieval accuracy [11]. The dual-pol antenna also provides the possibility to examine fully polarimetric GNSS-R system. Based on CYGNSS calibration experience, methods will be

Authorized licensed use limited to: University of Michigan Library. Downloaded on November 26,2024 at 16:43:37 UTC from IEEE Xplore. Restrictions apply.

developed for Rongowai calibration to address the following challenges: 1) Measurement of the GNSS cross-pol component, 2) calibration of the NGRx antenna pattern.

2. METHODOLOGY

Coherent polarimetric (LHCP and RHCP) signals reflected from inland waterbody with calm surface are measured by the Rongowai NGRx sensor, then compared with model results to calibrate dual-pol antenna pattern and GNSS-R cross-pol power measurement.

A matrix form of the Friis transmission formula is used to account for the coherent dual-pol signal reflection through the specular point, as given by

$$\begin{bmatrix} P_L \\ P_R \end{bmatrix} = \frac{\lambda^2}{(4\pi)^2 (R_1 + R_2)^2} \bar{\bar{G}} \bar{\bar{R}} \bar{E} |\chi|^2 \quad (1)$$

where

$$\bar{\bar{G}} = \begin{bmatrix} G_{LL} & G_{LR} \\ G_{RL} & G_{RR} \end{bmatrix}, \ \bar{\bar{R}} = \begin{bmatrix} R_{LR} & R_{LL} \\ R_{RR} & R_{RL} \end{bmatrix}, \ \bar{E} = \begin{bmatrix} E_R^{GNSS} \\ E_L^{GNSS} \end{bmatrix}$$

are the polarimetric antenna gain matrix, reflectivity matrix, and GNSS EIRP vector respectively. In equation (1), P is the received power, E is GPS effective instantaneous radiated power (EIRP), R_1 and R_2 are the distance between Transmitter-to-Specular and Receiver-to-Specular respectively, χ accounts for the scattering loss caused by surface roughness, and the subscripts denote the polarization state (L for LHCP, R for RHCP) of the signal. The surface Fresnel reflectivity in polarization LR/RL (Co-pol) and LL/RR (Cross-pol) are:

$$R_{LR} = R_{RL} = \left| \frac{1}{2} (R_{VV} - R_{HH}) \right|^2 \quad (2)$$

$$R_{LL} = R_{RR} = \left| \frac{1}{2} (R_{VV} + R_{HH}) \right|^2 \quad (3)$$

where

$$R_{VV} = \frac{\epsilon \cos\theta_i - \sqrt{\epsilon - \sin^2\theta_i}}{\epsilon \cos\theta_i + \sqrt{\epsilon - \sin^2\theta_i}} \quad (4)$$

$$R_{HH} = \frac{\cos\theta_i - \sqrt{\epsilon - \sin^2\theta_i}}{\cos\theta_i + \sqrt{\epsilon - \sin^2\theta_i}} \quad (5)$$

are the linear polarized Fresnel reflection coefficients, which are a function of the surface relative complex permittivity ϵ and incidence angle θ_i. For water surface, ϵ can be estimated through a microwave ocean dielectric model [12] as a function of salinity, temperature, and frequency. For inland waterbody, 0 salinity and 20°C are assumed.

The scattering loss caused by surface roughness is directly related to waterbody surface windspeed. Due to roughness, the received coherent power at the specular direction is attenuated by a factor [13]

$$|\chi|^2 = \exp(-4R_a^2) \quad (6)$$

where the Rayleigh parameter

$$R_a = \frac{\pi H_s \cos\theta_i}{2\lambda} \quad (7)$$

and H_s is the significant wave height which depends on windspeed, water depth, and fetch. The CERC empirical model [14] is used to calculate H_s.

The reflectivity model is used to predict coherent reflected power from Lake Taupo, the largest lake in New Zealand North Island, and compare with NGRx flight measurements during the calibration period from 10/27/2022 to 4/4/2023 (for 1ms coherent integration time) and from 4/16/2023 to 11/13/2023 (for 2ms coherent integration time) to examine and calibrate the NGRx measured dual-pol power. The lake surface windspeed is recorded hourly in the Turangi 2 EWS (#25643) station at the south coast of Lake Taupo. The windspeed data is released by NIWO Cliffo Service. A mean lake surface windspeed of 2.97 m/s is measured over the calibration period. A mean water depth of 110 m and a mean fetch of 2000 m are input into the CERC model to calculate the significant wave height and the scattering loss. With other Rongowai parameters, P_L and P_R can be estimated.

3. CALIBRATION RESULTS

The NGRx polarimetric power model and the flight measurements are compared to calibrate 1) NGRx polarimetric antenna pattern; and 2) dual-channel power bias.

3.1. Antenna Pattern

The gain pattern of the dual-pol Antenna deployed in the Rongowai mission was measured in the ElectroScience Lab from the Ohio State University. The chamber measured antenna LHCP cross-pol ratio (G_{LL}/G_{RL}) is plotted in figure 1 left. For signals reflected from inland water body with a smooth surface (assuming low cross-pol reflectivity and low GNSS cross-pol EIRP), then $P_L/P_R \approx G_{LL}/G_{RL}$. However, compared with the NGRx measured power cross-pol ratio from inland water surface plotted in Figure 1 right, a rotation of the pattern is observed. Here we apply a rotation to the antenna cross-pol pattern to remove the model-measurement bias. The root mean square difference (RMSD) between model and measurement is calculated, and a minimum RMSD is achieved after rotating the antenna pattern by 51° counterclockwise. This rotation is also applied in the following power calibration.

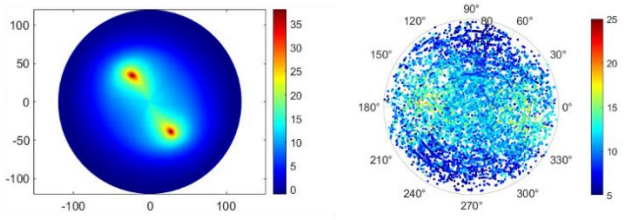


Figure 1 Left: Chamber measured NGRx antenna Xpol ratio at 1.575 GHz. Right: NGRx measured power cross-pol ratio from inland lake.

Authorized licensed use limited to: University of Michigan Library. Downloaded on November 26,2024 at 16:43:37 UTC from IEEE Xplore. Restrictions apply.

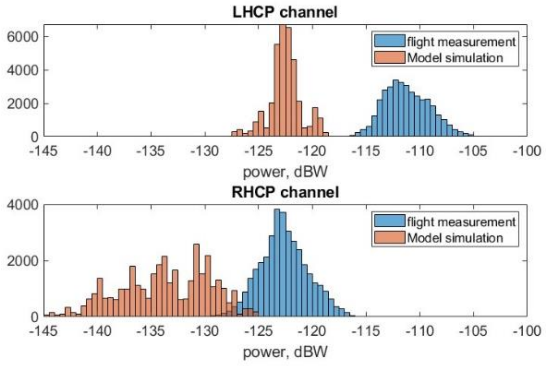


Figure 2 NGRx measured power (blue) vs modeled power (orange). Upper: LHCP Co-pol Channel; Lower: RHCP Cross-pol Channel

3.1. Level 1 Power Calibration

A bias is observed between modeled and measured specular power distribution in both co-pol (LHCP) and cross-pol (RHCP) Channels, as shown in figure 2.

Here we attempt to correct the measured power empirically by shifting it by a scale factor, and then compare the result with the reflectivity model by calculating their root mean square difference (RMSD). However, there are still three uncertainties in our model: windspeed, GPS cross-pol EIRP, antenna pattern change. While the average windspeed over the calibration period is used, the actual windspeed associated with each sample is unknown. Previous works [15] have indicated that GPS cross-pol EIRP might vary between 0 to 1% (-20 dB) of Co-pol EIRP, depending on the GPS block types, but there is no available measurement data for GPS cross-pol EIRP. In addition, we have lower confidence in the cross-pol leakage level in the low cross-pol isolation region of the antenna. This will result in inconsistent RMSD curves based on different assumptions about those uncertain quantities. Hence, we examine the RMSD curves with the following four conditions:

- Condition 1: off boresight angle < 60 deg
- Condition 2: condition 1 + Antenna xpol iso > 12 dB
- Condition 3: condition 2 + 1% GPS X-pol EIRP
- Condition 4: condition 1 + Antenna xpol iso < 10 dB

Note that windspeed variation is not tested since the attenuation of scattering loss caused by a mean windspeed in equation (1) on modeled power are the same for the above four conditions. The corresponding RMSD curves for 1 ms and 2 ms data, and LHCP and RHCP channels, of the four conditions are plotted in figure 3.

The calibration is considered to be robust if the RMSD curves are insensitive to changes is the uncertain parameters in the model. We observe that the RMSD curves for LHCP channel are similar, while the curves for RHCP channel are clearly inconsistent with each other. This is because: 1) the SNR of the cross-pol channel is much lower than that of the co-pol channel, which means that the cross-pol channel is more sensitive to noise; and 2) the cross-pol channel power is significantly affected by the power leakage from the co-pol channel due to the antenna cross-pol gain which might be corrupted. In addition, comparing condition 2 and 3, 1% GPS xpol EIRP is seen to have little impact on the co-pol channel's RMSD curve, but it changes cross-pol channel's RMSD curve significantly.

The strategy to calibrate the LHCP and RHCP channels is: 1) Assume the biases in both co- and cross-pol channels are the same; 2) Calibrate the co-pol power channel with different condition; and 3) Find an optimal power correction for the co-pol channel and apply same calibration to the cross-pol channel. Based on the results shown in Figure 3, the calibration for the co-pol channel is robust under different conditions. The power correction factors that achieve minimum RMSD for the four conditions are tabulated in table 1. We also note that there is a bias between 1 ms and 2 ms data, which might result from systematic difference, which may be verified later when other higher coherent integration time data become available. The fact that the RMSD curves under condition 4 are biased more than those for other conditions might result from the uncertainties in the low antenna cross-pol isolation portion of the pattern (most parts only have an isolation of ~5 dB), so the results for condition 4 were discarded. Averaging the data for different conditions, we obtain 11.83 dB and 13 dB for 1 ms and 2 ms coherent integration time conditions.

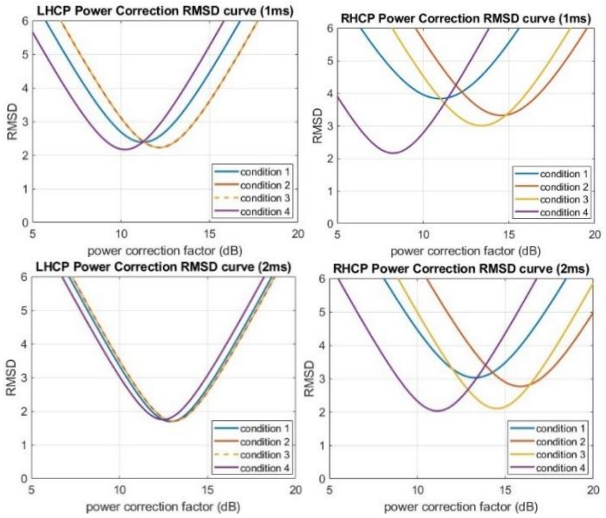


Figure 3 Upper Left: 1 ms LHCP, Upper right: 1 ms RHCP, Lower Left: 2 ms LHCP, Lower Right: 2 ms RHCP power correction RMSD curve

4. CONCLUSIONS AND FUTURE WORK

In this work, the NGRx antenna cross-pol pattern and its dual-pol channel power bias are calibrated. A polarimetric coherent reflection power model is developed and compared with the Rongowai flight polarimetric measurements over Lake Taupo in New Zealand to calibrate the polarimetric

Authorized licensed use limited to: University of Michigan Library. Downloaded on November 26,2024 at 16:43:37 UTC from IEEE Xplore. Restrictions apply.

NGRx sensor. A rotation is applied to the antenna pattern to make it consistent with the measured pattern of cross-pol power over inland waterbody. A power bias correction factor is derived and applied to both co- and cross-pol channels to calibrate the polarimetric power measurements. Results show that the minimum RMSD between model and measurement is achieved when 11.83 dB and 13 dB are applied to 1 and 2 ms coherent integration time measurements, respectively. After calibrating the absolute power measurement of the system, geophysical properties such as reflectivity and NBRCS can be retrieved accurately for future science applications.

The NGRx system has been operated with 1, 2, 4, 8, 16 ms coherent integration time processing. With higher coherent integration time, the SNR of both co- and cross-pol channels is observed to increase, and we expect the system to capture better cross-pol signals scattered from various types of earth surfaces, and to improve the cross-pol channel calibration.

Table 1 Power Correction Factor under different conditions

	Power Correction Factor (dB)	
	1 ms	***2 ms***
Condition 1	11.4	12.9
Condition 2	12.1	13.1
Condition 3	12	13
Condition 4	10.5	12.5

5. REFERENCES

[1] Gleason, S., "Remote Sensing of Ocean, Ice and Land Surfaces Using Bistatically Scattered GNSS Signals from Low Earth Orbit," Ph.D. diss., University of Surrey, UK, 213 pp, 2006

[2] Unwin, M., P. Jales, J. Tye, C. Gommenginger, G. Foti, J. Rosello, "Spaceborne GNSS-Reflectometry on TechDemoSat-1: Early Mission Operations and Exploitation," IEEE J. Sel. TOp. Appl. Earth Obs. Remote Sens., 9(10), 4525-4539, doi: 10.1109/JSTARS.2016.2603846, 2016.

[3] Ruf, C. S., R. Atlas, P. S. Chang, M. P. Clarizia, J. L. Garrison, S. Gleason, S. J. Katzberg, Z. Jelenak, J. T. Johnson, S. J. Majumdar, A. O'Brien, D. J. Posselt, A. J. Ridley, R. J. Rose, V. U. Zavorotny, "New Ocean Winds Satellite Mission to Probe Hurricanes and Tropical Convection," Bull. Amer. Meteor. Soc., doi:10.1175/BAMS-D-14-00218.1, pp385-395, Mar 2016

[4] Clarizia, M. P., and C. S. Ruf, "Wind Speed Retrieval Algorithm for the Cyclone Global Navigation Satellite System (CYGNSS) Mission," IEEE Trans Geosci. Remote Sens., 54(8), doi:10.1109/TGRS.2016.2541343, 2016

[5] Wang, T., C. S. Ruf, S. Gleason, A. J. O'Brien, D. S. McKague, B. P. Block, A. Russel, "Dynamic Calibration of GPS Effective Isotropic Radiated Power for GNSS-Reflectometry Earth Remote Sensing," IEEE Trans. Geosci. Remote Sens., doi: 10.1109/TGRS.2021.3070238, 2021

[6] Wang, T., C. S. Ruf, B. Block, D. S. McKague, S. Gleason, "Design and Performance of a GPS Constellation Power Monitor System for Improved CYGNSS L1B Calibration," IEEE J. Sel. Topics Appl. Earth Obs. Remote Sens., doi: 10.1109/JSTARS.2018.2867773, 2018

[7] Jensen, K., K. McDonald, E. Podest, N. Rodriguez-Alvarez, V. Horna, N. Steiner, "Assessing L-Band GNSS-Reflectometry and Imaging Radar for Detecting Sub-Canopy Inundation Dynamics in a Tropical Wetlands Complex," Remote Sensing, DOI:10.3390/rs10091431, 2018

[8] Garrison, J.L. and S.J. Katzberg, "Effect of sea roughness on bistatically scattered range coded signals from the Global Positioning System," Geophysical Research Letters, Vol. 25, No.13, pp 2257-2260, July 1, 1998

[9] Garrison, J. L., A. Komjathy, V. U. Zavorotny and S. J. Katzberg, "Wind Speed Measurement Using Forward Scattered GPS Signals," IEEE Transactions on Geoscience and Remote Sensing, Vol. 40, No. 1, January 2002

[10] Moller, D., C. Ruf, R. Linnabury, A. O'Brien, S. Musko, "Operational Airborne GNSS-R Aboard Air New Zealand Domestic Aircraft," Proc. 2021 International Geoscience and Remote Sensing Symposium, virtual, doi: 10.1109/IGARSS47720.2021.9553159, 2021

[11] Ruf. C., R. Backhus, T. Butler, C. Chen, S. Gleason, E. Loria, D. McKague, R. Miller, A. O'Brien, L. van Nieuwstadt, "Next Generation GNSS-R Instrument," Proc. 2020 International Geoscience and Remote Sensing Symposium, virtual, doi: 10.1109/IGARSS39084.2020.9324588, Oct 2020

[12] L. Klein and C. Swift, "An improved model for the dielectric constant of sea water at microwave frequencies," in IEEE Journal of Oceanic Engineering, vol. 2, no. 1, pp. 104-111, January 1977, doi: 10.1109/JOE.1977.1145319.

[13] David Long; Fawwaz Ulaby, Microwave Radar and Radiometric Remote Sensing, Artech, 2015.

[14] E. Loria, A. O'Brien, V. Zavorotny and C. Zuffada, "Wind Vector and Wave Height Retrieval in Inland Waters Using CYGNSS," IGARSS 2020 - 2020 IEEE International Geoscience and Remote Sensing Symposium, Waikoloa, HI, USA, 2020, pp. 7029-7032, doi: 10.1109/IGARSS39084.2020.9323481.

[15] Wu, Andy, "Predictions and Field Measurements of the GPS Block IIR L1 and L2 Ground Powers," Proceedings of the 2002 National Technical Meeting of The Institute of Navigation, San Diego, CA, January 2002, pp. 931-938.

Authorized licensed use limited to: University of Michigan Library. Downloaded on November 26,2024 at 16:43:37 UTC from IEEE Xplore. Restrictions apply.